Monochromatic x-ray backlighting of wire-array *z*-pinch plasmas using spherically bent quartz crystals

D. B. Sinars,[a] M. E. Cuneo, G. R. Bennett,[b] D. F. Wenger, L. E. Ruggles, M. F. Vargas, J. L. Porter, R. G. Adams, D. W. Johnson, K. L. Keller, P. K. Rambo, D. C. Rovang, H. Seamen,[b] W. W. Simpson, I. C. Smith,[c] and S. C. Speas
Sandia National Laboratories, P. O. Box 5800, Albuquerque, New Mexico 87185-1193

(Presented on 11 July 2002)

X-ray backlighting systems are being developed to diagnose *z*-pinch, inertial confinement fusion capsule, and complex hydrodynamics experiments on the 20 MA Sandia *Z* machine. The x-ray backlighter source is a laser-produced plasma created using the *Z*-Beamlet laser, a 2 TW, 2 kJ Nd:glass laser recently constructed at Sandia. As an alternative to point-projection radiography, we are investigating a different geometry [S. A. Pikuz *et al.*, Rev. Sci. Instrum. **68**, 740 (1997)] that uses spherically bent crystal mirrors to simultaneously obtain high spatial resolution and a narrow spectral bandwidth. Backlighting systems using the Si He_α line (1.865 keV) and the Mn He_α line (6.15 keV) are discussed. These systems are capable of spatial resolutions in the 5–10 μm range, a field of view as large as 5 mm by 20 mm, and a spectral bandwidth comparable to the width of the emission line used for backlighting. © *2003 American Institute of Physics.*
[DOI: 10.1063/1.1537853]

I. INTRODUCTION

The *Z* machine at Sandia National Laboratories, Albuquerque,[1] is a 20 MA, 100 ns rise-time, pulsed-power driver for *z*-pinch plasma radiation sources. The current from the driver is passed through a cylindrical array of wires, which vaporize and form plasma, and the magnetic forces compress the plasma to the axis of the system. This technique has successfully been used to generate a 200 TW, 2 MJ plasma radiation source with a near-blackbody spectral shape.[2] This radiation source can be used as a driver for fusion experiments,[3–7] radiation effects testing, or complex hydrodynamics experiments similar to those in Ref. 8.

Z-Beamlet,[9] a 2 TW, 2 kJ Nd:glass laser, became operational in 2001 and was used to diagnose high-yield-fusion capsule implosions in a hohlraum driven on two sides by *z* pinches.[6,10] In these tests, the laser beam was focused onto Ti or Fe targets to produce 4.5 or 6.7 keV x rays, respectively, which were used to backlight the capsules in a point-projection geometry. For the point-projection geometry to succeed, the x-ray background produced by the *z* pinches had to be eliminated. The soft (<1 keV) x rays were eliminated using filters and hard (>10 keV) x rays were reduced by carefully collimating the detector to a 3 mm field of view centered on a capsule located no closer than 6.5 mm from the ends of either pinch.[6] Collimating out the hard x rays when directly imaging the *z*-pinch implosion is difficult, though it is possible to obtain a one-dimensional image using a 250 μm slit at large radius.

To eliminate the hard x-ray background, we used spherically bent crystals in an x-ray backlighting geometry originally proposed by Pikuz *et al.*[11,12] Only x rays satisfying the Bragg condition,

$$n\lambda = 2d \sin\theta, \tag{1}$$

reflect constructively from the surface of the crystal, where λ is the incident photon wavelength, d is the spacing of planes in the crystal, θ is the "grazing" angle (the angle with respect to the crystal plane), and n is an integer corresponding to the crystal reflection order. In this way, both the soft and hard x-ray background from sources within the field of view of the backlighter can be eliminated, and the backlighter system can readily be considered "monochromatic."

A second advantage of this backlighting geometry is that it can be used to obtain images with <10 μm spatial resolution. For example, a monochromatic backlighting system based on the Si He_α line recently demonstrated 3–5 μm spatial resolution.[13,14] This system was used to measure the ablative Richtmyer–Meshkov instability for the first time.[15,16] A third advantage is that the spatial resolution is only weakly dependent on the size of the x-ray source,[17] which means that relatively large sources ($\geqslant 100$ μm) can be used. By contrast, to obtain ~ 10 μm resolution with a point-projection system, the system must either use a small source at low magnification or use a pinhole to reduce the size of the source (at a cost of x-ray flux).

The design of monochromatic backlighting systems with parameters relevant to the *Z* machine was considered in a separate publication.[17] On the basis of these estimates, systems using Si He_α line at 1.865 keV and the Mn He_α line at 6.15 keV were built. We present the results of calibration tests of both of these systems carried out using the *Z*-Beamlet laser. Results from the first wire-array backlight-

[a]Electronic mail: dbsinar@sandia.gov
[b]Also at: Ktech Corp., 2201 Buena Vista SE, Suite 400, Albuquerque, NM 87106-4625.
[c]Also at: Atomic Weapons Establishment, Reading, UK.

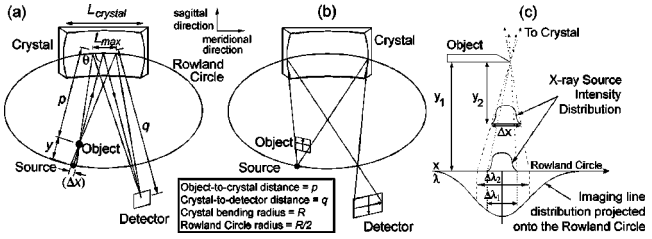

FIG. 1. Schematic diagrams illustrating the monochromatic backlighting concept, emphasizing (a) the effect of the source size on the collection angle of the system and (b) the effect of the crystal size in determining the available field of view. (c) If the x-ray source is on the Rowland circle, its width Δx determines the spectral bandpass used for imaging ($\Delta\lambda_1$), which is usually less than the width of the spectral emission line. Moving the source off the Rowland circle can effectively increase the spectral bandpass of the system as shown to $\Delta\lambda_2$, thereby increasing the efficiency of the system.

ing experiment using the 1.865 keV system are also briefly discussed.

II. MONOCHROMATIC X-RAY BACKLIGHTING TECHNIQUE

A generic x-ray backlighting system using a spherically bent crystal is shown in Fig. 1. The behavior of this optical system is governed by two general principles: The Bragg condition in Eq. (1) and the concept of the Rowland circle. The Rowland circle has a radius $R/2$, where R is the bending radius of the crystal. Rays from a point located on the Rowland circle are focused to a corresponding point on the other side of the circle (across the line of normal incidence), as seen in Fig. 1(b). Because of the Bragg reflection properties of the crystal, however, only rays from the source satisfying the Bragg condition are focused back onto the Rowland circle. If an object is placed along the path of these rays a distance p from the crystal, where p satisfies

$$R_m \sin\theta > p > \frac{R_m}{2}\sin\theta, \tag{2}$$

a detector can be placed at the focal point of the object so that a monochromatic image of the object is obtained.[11]

The focal points for the horizontal (meridional) and vertical (sagittal) planes of the crystal are

$$\frac{1}{p}+\frac{1}{q_m}=\frac{2}{R_m\sin\theta}, \tag{3}$$

$$\frac{1}{p}+\frac{1}{q_s}=\frac{2\sin\theta}{R_s}, \tag{4}$$

respectively. If $R_s=R_m\sin^2\theta$ (i.e., a toroidally bent crystal is used), then $q_s=q_m$ and astigmatism is reduced to a minimum. Alternatively, $q_s=q_m$ also occurs if $\theta=90°$. If θ is in the range from 80° to 90°, however, then a spherical crystal ($R_s=R_m$) can be used with a relatively small amount of astigmatism sufficient to obtain μm-scale spatial resolution.[11] Thus, in this range, there is little difference in the performance of spherically and toroidally bent crystals. For Bragg angles $<80°$, toroidally bent crystals are preferred in principle, but in practice higher-order aberrations and x-ray diffraction effects often negate the advantage and such crystals are difficult to work with.

The magnifications in the meridional and sagittal planes are

$$M_m=\frac{q-R\sin\theta}{R\sin\theta-p}, \tag{5}$$

$$M_s=\frac{q}{p}, \tag{6}$$

respectively. For a toroidally bent crystal, $q=q_m=q_s$, so $M_s=M_m$. For a spherically bent crystal, $M_s=M_m$ only if the detector distance $q=q_m$ in Eq. (3), which is what we used to determine the detector position in these experiments. From Eqs. (3) and (6), one can also derive the following relationship to determine the object position for a given crystal and desired magnification:

$$p=\frac{(R\sin\theta)(M+1)}{2M}. \tag{7}$$

As noted elsewhere,[13,14] it is not necessary for the backlighting source to lie on the Rowland circle. If the x-ray source is moved inside of Rowland circle the spectral bandwidth and collection solid angle both increase, as illustrated in Fig. 1(c), making the system more efficient. The penalty is a reduced field of view and worse spatial resolution. Calculations illustrating this are presented elsewhere.[17] This was done with the Mn He_α system to increase the flux at the detector by 17 times.

The field of view (FOV) of the backlighting system can be estimated by

$$\mathrm{FOV}=L_{\mathrm{crystal}}\left\{\frac{y}{p+y}\right\}, \tag{8}$$

where L_{crystal} is the width of the crystal in the meridional or sagittal direction and y is the distance from the source to the object. This equation holds for sources both on and inside the Rowland circle.

III. *Z*-BEAMLET CALIBRATION TESTS

Tests of 1.865 and 6.15 keV monochromatic backlighting systems were carried out in a calibration chamber for the *Z*-Beamlet laser. The parameters of these test systems, summarized in Table I, were chosen with the backlighting requirements for experiments on the *Z* machine in mind. Additional details of these designs can be found in Ref. 17. Note that in the Mn He_α system the source was located 63 mm inside the Rowland circle to increase the flux reaching the detector by 17 times.

The object in these experiments was an electroformed Ni mesh with 33.5 μm rectangular wires (5 μm thick) spaced every 318 μm. Sample images from these tests, along with a sample lineout through one wire, are shown in Fig. 2. The Si He_α system was designed for a spatial resolution of about 10 μm, and the Mn He_α system for a spatial resolution of about 6 μm.[17] The experimentally measured spatial resolution varied from 9 to 13 μm for the Si He_α system (center to edge), and from 10 to 12 μm for the Mn He_α system (center to edge).

TABLE I. A summary of the parameters of the Si He_α and Mn He_α backlighting systems tested using the *Z*-Beamlet laser. The bending radius of the crystals was 250 mm.

Emission line	Si He_α	Mn He_α
Source wavelength (Å)	6.65	2.016
Crystal	Quartz $10\bar{1}1$	Quartz $22\bar{4}3$
Reflection order	1	1
Integrated reflectivity (mrad)	~1	0.078
Bragg angle (°)	83.9	84.9
Crystal size (mm)	48×11	23 (diameter)
Object to crystal distance (mm)	145	145
Source to object distance (mm)	104	40
Field of view (mm)	20×5	5 (diameter)
Detector film (Kodak)	RAR 2497	DEF
Laser pulse width (ns)	0.6	1.0
Laser energy (J)	400–600	1000
Laser spot size (mm)	0.8	0.15

IV. *Z*-MACHINE EXPERIMENTS

The backlighter systems were designed as diagnostics for wire-array implosions. The narrow spectral range passed by these systems is important when diagnosing intense x-ray sources such as a 200 TW *z*-pinch blackbody. However, though the spectral bandwidth for the Si He_α system is <1 mÅ, the radiation in this range reaching the crystal from such a *z* pinch is comparable to that produced by the backlighter. By contrast, the intensity of the 6.15 keV backlighter source in the Mn He_α system exceeds that produced by a *z* pinch. Thus, the Si He_α system is appropriate for looking at large radii, while the Mn He_α system could potentially be used to look directly at the *z* pinch itself.

The first Si He_α tests studied the implosion of cylindrical tungsten wire arrays that were 20 or 12 mm in diameter. Recent work suggests that not all of the mass accelerates to the axis during the implosion, but that some of the mass is ''left behind'' near the original location of the wire arrays.[18,19] One goal of the Si He_α backlighter was to directly measure the presence of any mass left behind. The wire-array hardware for these tests was designed to allow a field of view suitable for such measurements, as discussed in Fig. 3. Though the field of view shown in Fig. 3 extends all the way to the axis of the system, during the experiments a 75 μm thick Au foil was placed over the inner 2 mm of the exit aperture to prevent x rays from the *z* pinch from reaching the detector. The detector (film) was placed inside a collimated tungsten/stainless-steel housing as shown in Fig. 4. In addition, two tungsten blocks were placed in the direct line of sight between the film and the *z*-pinch source. X rays reflected from the crystal pass through a 2 mm aperture in one of the tungsten blocks, and the line of sight between this aperture and the return-current can was blocked using the second tungsten piece.

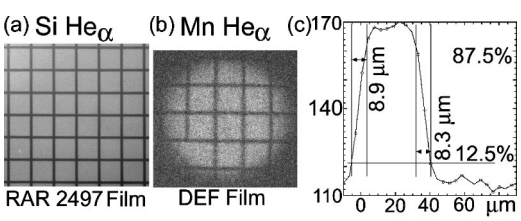

FIG. 2. Test images of a 33.5 μm Ni mesh obtained using (a) the Si He_α and (b) the Mn He_α backlighting systems. (c) A sample lineout through a portion of the Ni mesh image in (a).

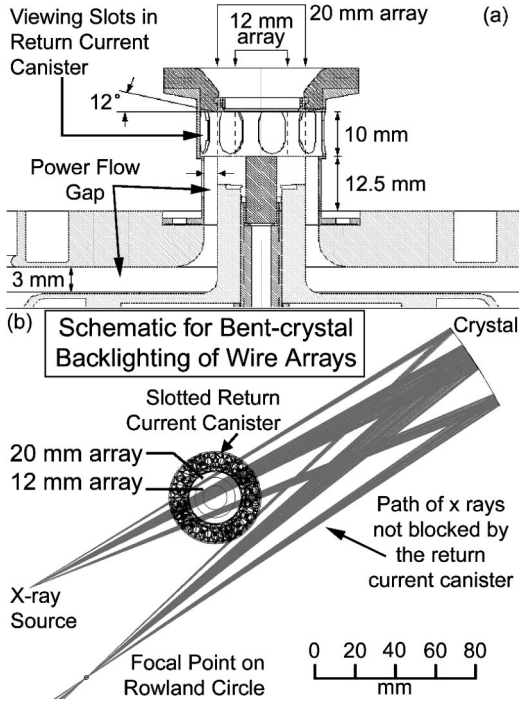

FIG. 3. (a) Schematic diagram of the wire-array hardware. In these tests, the center of the wire array is 17.5 mm above the horizontal plane to accomodate the existing detector hardware. There are nine slots in the return-current canister for diagnostic access. Using the ZEMAX ray-tracing program (see Ref. 20) to simulate the Si He_α geometry, the width of the slots was adjusted to obtain the desired field of view of the 20 and 12 mm wire arrays being tested. The circles inside the canister in (b) indicate the positions of these arrays.

On July 5, 2002, the Si He_α system was fielded on a *Z*-machine shot for the first time. The load on this test was a 12 mm diameter, 10 mm tall, 180 W wire array, so only the center image of the object (from $r=6$ mm to $r=2$ mm) was expected to contain data. The film from this test is shown in

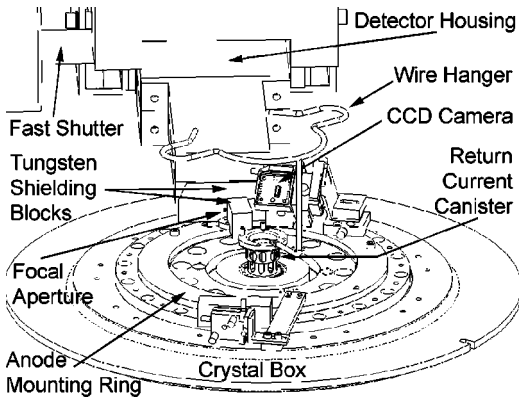

FIG. 4. A diagram of the *Z*-machine hardware for the Si He_α backlighting system. A charge coupled device camera is used to align the focal spot of the laser beam on a target foil (not shown) mounted on the sloped face of the tungsten shielding block. The crystal focuses the source x rays through a 2 mm aperture in one of two tungsten shielding blocks. The second block is used to eliminate the direct line of sight between the return-current can and the aperture. A fast-closing shutter mounted in the detector housing prevents debris from reaching the film.

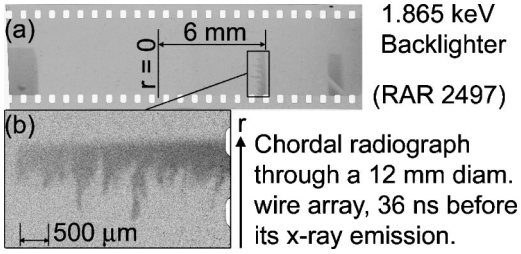

FIG. 5. (a) Sample film result from *Z*-machine test z931. The load was a 12 mm diameter, 180 W wire array. The image was made 36 ns before the peak *z*-pinch x-ray emission. (b) An expanded view of the central slot image, showing the complex axial and radial mass distribution.

Fig. 5. The image, taken about 36 ns before peak x-ray emission, shows a nonuniform axial and radial mass distribution in the imploding pinch. A detailed analysis of the image is pending.

ACKNOWLEDGMENTS

This work was performed for the United States Department of Energy by Sandia National Laboratories under Contract No. DE-AC04-94AL85000. Sandia is a multiprogram laboratory operated by Sandia Corporation, a Lockheed–Martin Company.

[1] R. B. Spielman *et al.*, *Proceedings of the 11th International Conference on High-Power Particle Beams, Prague, Czech Rep., 1996*, edited by K. Jungwirth and J. Ullschmied (Czech Academy of Sciences, Prague, 1996), Vol. 1, p. 150.
[2] R. B. Spielman *et al.*, Phys. Plasmas **5**, 2105 (1998).
[3] R. J. Leeper *et al.*, Nucl. Fusion **39**, 1283 (1999).
[4] M. E. Cuneo *et al.*, Phys. Plasmas **8**, 2257 (2001).
[5] T. W. L. Sanford *et al.*, Phys. Rev. Lett. **83**, 5511 (1999).
[6] G. R. Bennett *et al.*, Phys. Rev. Lett. (to be published).
[7] D. L. Hanson *et al.*, Phys. Plasmas **9**, 2173 (2002).
[8] J. M. Foster, B. H. Wilde, P. A. Rosen, T. S. Perry, M. Fell, M. J. Edwards, B. F. Lasinski, R. E. Turner, and M. L. Gittings, Phys. Plasmas **9**, 2251 (2002).
[9] P. K. Rambo *et al.*, *Proceedings of the Conference on Lasers Electro-Optics, Long Beach, CA* (Optical Society of America, Washington, DC, 2002), pp. 362–363.
[10] M. E. Cuneo *et al.*, Phys. Rev. Lett. **88**, 215004 (2002).
[11] S. A. Pikuz, T. A. Shelkovenko, V. M. Romanova, D. A. Hammer, A. Y. Faenov, V. A. Dyakin, and T. A. Pikuz, Rev. Sci. Instrum. **68**, 740 (1997).
[12] S. A. Pikuz, T. A. Shelkovenko, V. M. Romanova, D. A. Hammer, A. Y. Faenov, V. A. Dyakin, and T. A. Pikuz, JETP Lett. **61**, 638 (1995).
[13] Y. Aglitskiy *et al.*, Appl. Opt. **37**, 5253 (1998).
[14] Y. Aglitskiy, T. Lehecka, S. Obenschain, C. Pawley, C. M. Brown, and J. Seely, Rev. Sci. Instrum. **70**, 530 (1999).
[15] Y. Aglitskiy, A. L. Velikovich, M. Karasik, V. Serlin, C. J. Pawley, A. J. Schmitt, S. P. Obenschain, A. N. Mostovych, J. H. Gardner, and N. Metzler, Phys. Rev. Lett. **87**, 265001 (2001).
[16] Y. Aglitskiy, A. L. Velikovich, M. Karasik, V. Serlin, C. J. Pawley, A. J. Schmitt, S. P. Obenschain, A. N. Mostovych, J. H. Gardner, and N. Metzler, Phys. Rev. Lett. **87**, 265002 (2001).
[17] D. B. Sinars, G. R. Bennett, D. F. Wenger, M. E. Cuneo, and J. L. Porter (to be published).
[18] M. E. Cuneo *et al.*, Bull. Am. Phys. Soc. **46**, 235 (2001).
[19] S. V. Lebedev *et al.*, Phys. Plasmas **8**, 3734 (2001).
[20] ZEMAX Optical Design Program, ZEMAX Development Corp., 4901 Morena Blvd., Suite 207, San Diego, CA 92117-7320.